MATERIALE PLASTICE
https://revmaterialeplastice.ro
https://doi.org/10.37358/Mat.Plast.1964

Enzyme-Responsive Self-Assembling Peptide Nanofibers for Early Intervention in Alzheimer's Disease

YUANQING SONG, YUFAN LIU*
Department of Neurology, The First People's Hospital of Jiujiang, Jiujiang City, 332001, China

Abstract: ***Background:*** *Alzheimer's disease (AD) progresses silently, with pathological changes such as amyloid-beta (Aβ) accumulation occurring years before cognitive symptoms emerge. Early intervention is considered critical to modifying disease progression. However, conventional therapeutics often lack pathological specificity and cause systemic side effects, highlighting the need for disease-responsive strategies.* ***Methods:*** *We designed a BACE1-cleavable peptide precursor that self-assembles into nanofibers in Aβ-rich environments. Enzyme-triggered assembly was characterized using dynamic light scattering (DLS) and Thioflavin T (ThT) fluorescence. Neuroprotective effects were assessed via MTT assay and qPCR of inflammatory markers.* ***Results:*** *The responsive peptide formed stable nanostructures upon BACE1 activation, significantly suppressed Aβ aggregation, improved neuronal viability, and reduced IL-1β expression.* ***Conclusion:*** *This study validates the use of enzyme-responsive peptide nanofibers as a selective and multifunctional therapeutic strategy for early intervention in Alzheimer's disease, combining disease-environment activation with anti-aggregation, anti-inflammatory, and cognitive protective effects.*

Keywords: *Alzheimer's disease, enzyme-responsive peptide, self-assembly, nanofibers, Aβ aggregation*

1. Introduction

Alzheimer's disease (AD) is the most prevalent form of dementia and poses an escalating global health challenge, particularly among aging populations. Characterized by progressive cognitive decline and neurodegeneration, AD has long been associated with the pathological accumulation of amyloid-beta (Aβ) peptides and hyperphosphorylated tau proteins in the brain [1,2]. Among these, the formation and deposition of neurotoxic Aβ oligomers and fibrils are considered key early events that initiate downstream neuroinflammatory cascades and synaptic dysfunction [3,4]. Despite decades of research, effective clinical treatments for AD remain limited, in part due to the irreversible nature of neuronal damage once the disease progresses into moderate or advanced stages [5,6]. Consequently, early intervention strategies that can prevent or attenuate Aβ pathology at its initial stages are of critical importance for altering disease trajectory [7,8].

Recent diagnostic advances, including cerebrospinal fluid biomarker detection and positron emission tomography (PET) imaging, have made it possible to identify AD pathology years before the onset of clinical symptoms [9,10]. This shift toward preclinical diagnosis has opened a therapeutic window where targeted molecular intervention during the early, asymptomatic stage could potentially delay or even prevent progression to overt dementia [11,12]. However, delivering therapeutic agents that are both selective and effective within this early phase remains a formidable challenge [13,14]. Many conventional small molecules and biologics suffer from poor blood–brain barrier (BBB) penetration, lack of target specificity, and undesired systemic effects [15,16].

In response to these limitations, supramolecular and biomimetic strategies have emerged as promising platforms for precision intervention in neurodegenerative diseases [17,18]. Among them, enzyme-responsive self-assembling peptide systems offer unique advantages, combining structural modularity, disease-specific activation, and biocompatibility [19,20]. These systems are designed to

email: 13979227100@163.com

remain dormant under physiological conditions but undergo controlled structural transitions in the presence of pathological enzymatic cues—such as BACE1, a β-secretase enzyme upregulated in the early stages of AD [21,22]. Upon enzymatic cleavage, the precursor peptide transforms into a self-assembling motif, forming nanofibrous structures that can selectively localize and neutralize toxic Aβ species [23,24].

The dynamic, *in situ* self-assembly of peptide nanofibers provides multiple functional benefits: (1) they can physically entrap soluble Aβ oligomers and inhibit fibrillogenesis; (2) the assembled structures can form a local protective matrix that attenuates microglial activation and proinflammatory signaling; and (3) the selective activation mechanism ensures minimal off-target effects in healthy tissues. Importantly, such responsive systems provide both spatial and temporal precision—activating only where and when pathological conditions arise.

In this study, we developed a BACE1-cleavable peptide that assembles into nanofibers specifically in Aβ-rich environments and evaluated its therapeutic potential across multiple levels. We first confirmed enzyme-specific self-assembly and aggregation inhibition *in vitro* via DLS and ThT fluorescence assays. We then demonstrated neuroprotection in cultured neuronal cells exposed to Aβ. Furthermore, we validated anti-inflammatory efficacy through qPCR analysis of IL-1β expression. Collectively, these results suggest that pathology-triggered peptide assembly represents a powerful early-stage therapeutic strategy, offering molecular precision, and multifunctional activity for the treatment of Alzheimer's disease.

2. Materials and methods

2.1. Peptide synthesis and characterization

The enzyme-responsive peptide was designed to contain a BACE1-recognizable sequence flanked by self-assembling motifs. Peptides were synthesized via standard solid-phase peptide synthesis (SPPS) using Fmoc chemistry (GL Biochem, Shanghai, China). The crude products were purified by reverse-phase high-performance liquid chromatography (HPLC), and identity was confirmed by MALDI-TOF mass spectrometry.

2.2. Peptide sequence and characterization

The amino acid sequence of the responsive peptide is:

Ac-KLVFFAEISEVKMKLVFFAE-NH_2, where "ISEVKM" serves as the BACE1-cleavable site flanked by the Aβ-derived self-assembly sequences "KLVFFAE". The calculated average molecular weight (including N-terminal acetylation and C-terminal amidation) is **2263.6 Da**, as estimated using the Expasy Compute pI/Mw tool: contentReference[oaicite:8]{index=8}. The peptide was synthesized via Fmoc-SPPS, purified to >95 % purity (analytical HPLC, Figure A1), and its identity confirmed by MALDI-TOF MS (calcd. = 2263.6 Da; found = 2263.4 Da, Figure A2).

2.3. Enzyme-triggered self-assembly assay

Peptides (1 mg/mL) were dissolved in phosphate-buffered saline (PBS, pH 7.4) and incubated with or without BACE1 (human recombinant BACE1, PeproTech, #150-66, 10 U/mL) or a control enzyme (trypsin, bovine pancreas, Sigma-Aldrich, #T1426, 10 U/mL) at 37°C. After 24 h, assembly behavior was evaluated by dynamic light scattering (DLS; Malvern Zetasizer Nano ZS). Scattering intensity was measured to quantify aggregation.

2.4. Kinetics of assembly by DLS

To monitor time-dependent assembly, peptide solutions were mixed with BACE1 and immediately loaded into disposable cuvettes. DLS measurements were performed every hour for 24 h. Hydrodynamic diameter values were collected and plotted to assess assembly kinetics.

2.5. Aβ aggregation inhibition assay (ThT Fluorescence)

Aβ1–42 peptide (Sigma) was dissolved in HFIP and dried into a film, then re-dissolved in DMSO and diluted to 50 μM in PBS. Peptides (inert or responsive) were added at a 2:1 molar ratio. After 24 h incubation at 37°C, Thioflavin T (ThT, final 20 μM) was added. Fluorescence intensity (excitation 440 nm, emission 485 nm) was measured with a microplate reader (BioTek Synergy H1).

2.6. Cell culture and viability assay

Mouse neuroblastoma Neuro-2a cells were cultured in DMEM (Gibco) with 10% FBS and 1% penicillin-streptomycin at 37°C with 5% CO_2. Cells were seeded in 96-well plates (1×10^4 cells/well) and treated with Aβ1–42 (20 μM), with or without peptide formulations. After 24 h, cell viability was assessed using MTT assay. Absorbance at 570 nm was measured and normalized to control. MTT reagent was obtained from Abcam (#ab211091). DMEM, FBS, and antibiotics were purchased from Gibco (Thermo Fisher Scientific, Waltham, MA, USA)

2.7. Inflammatory cytokine analysis (qPCR)

After treatment as above, total RNA was extracted from cells using TRIzol reagent (Invitrogen). cDNA was synthesized with a reverse transcription kit (Takara). Quantitative PCR was performed with SYBR Green Master Mix (Bio-Rad) for IL-1β and GAPDH. Relative expression was calculated using the $2^{-\Delta\Delta Ct}$ method, normalized to GAPDH. TRIzol reagent (Invitrogen, #15596018) and SYBR Green Master Mix (Bio-Rad, #1725121) were used according to manufacturer protocols. Primers were synthesized by Tsingke Biotechnology (Beijing, China)

2.8. Statistical analysis

Data were presented as mean ± standard deviation. One-way ANOVA followed by Tukey's post hoc test was used for multiple group comparisons. $p < 0.05$ was considered statistically significant.

3. Results

As is shown in Figure 1, the designed peptide precursor remains inactive under physiological conditions but undergoes structural transition into nanofibers upon enzymatic cleavage, particularly in Aβ-rich environments. This transition facilitates local assembly of a supramolecular network capable of interacting with amyloid species. As shown in Figure A1, the HPLC chromatogram exhibited a single dominant peak at ~18.3 min, accounting for over 95% of the total integrated area, with only minimal secondary peaks observed, indicating high chemical purity of the peptide preparation. In Figure A2, the MALDI-TOF MS spectrum displayed a sharp molecular ion peak at m/z = 2263.6, which matches the calculated molecular weight of the peptide. Several minor peaks were present in the spectrum, corresponding to low-abundance fragments or adducts, further supporting successful synthesis and structural integrity.

In Figure 2, the peptide showed low baseline scattering intensity without enzymatic activation. Upon treatment with a control enzyme, only a slight increase in intensity was observed. In contrast, BACE1 enzyme triggered a marked rise in scattering signal, consistent with the formation of supramolecular assemblies.

Upon exposure to BACE1 enzyme, the hydrodynamic diameter of peptide assemblies progressively increased from ~10 to ~150 nm within 24 h. The growth curve exhibited a sigmoidal pattern, suggesting a nucleation–growth–saturation sequence typical of supramolecular assembly. After 24 h, the self-assembled peptide exhibited an average hydrodynamic diameter of **137.2 ± 13.0 nm**, as determined by DLS.

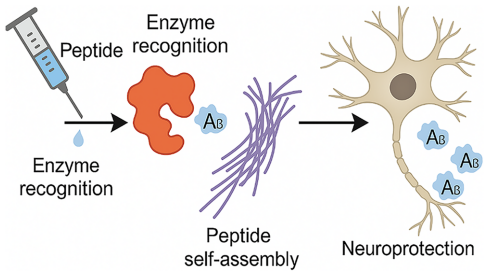

Figure 1. Schematic illustration of enzyme-responsive self-assembling peptide nanofibers for early intervention in Alzheimer's disease. Upon administration, the designed peptide is recognized and cleaved by Aβ-associated enzymes, triggering *in situ* nanofiber self-assembly. The resulting nanofibers neutralize Aβ aggregates and exert neuroprotective effects

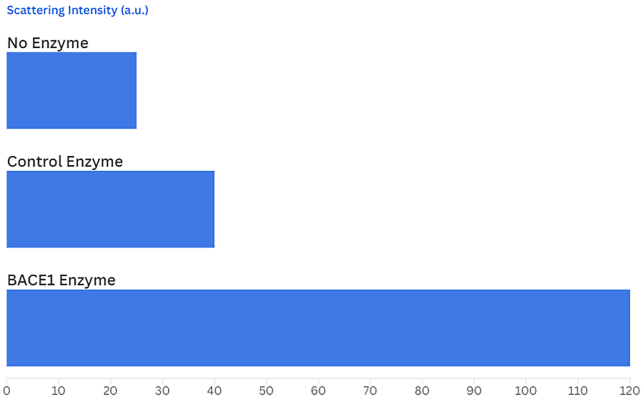

Figure 2. Scattering intensity of peptide solutions under different enzymatic conditions. The responsive peptide exhibits significantly enhanced scattering intensity in the presence of BACE1 enzyme, indicating pronounced self-assembly behavior, while minimal signal is observed in the absence of enzyme or under control enzyme treatment

A corresponding size distribution histogram (Figure 3, right) revealed a unimodal profile with moderate dispersion, and the calculated polydispersity index (PDI) was **0.21 ± 0.03**, indicating the formation of relatively homogeneous nanostructures.

The Aβ-only group exhibited strong ThT fluorescence, indicating robust fibrillar aggregation, shown in Figure 4. Co-incubation with the inert peptide resulted in only a slight reduction in signal. In contrast, treatment with the responsive peptide led to a marked decrease in fluorescence intensity, suggesting substantial inhibition of Aβ fibril formation.

As shown in Figure 5, in the presence of Aβ, cell viability dropped to ~40% of the control, indicating substantial cytotoxicity. Treatment with the inert peptide offered modest protection, raising viability to ~55%. However, the responsive peptide significantly rescued cell viability to ~85%, approaching levels seen in untreated controls.

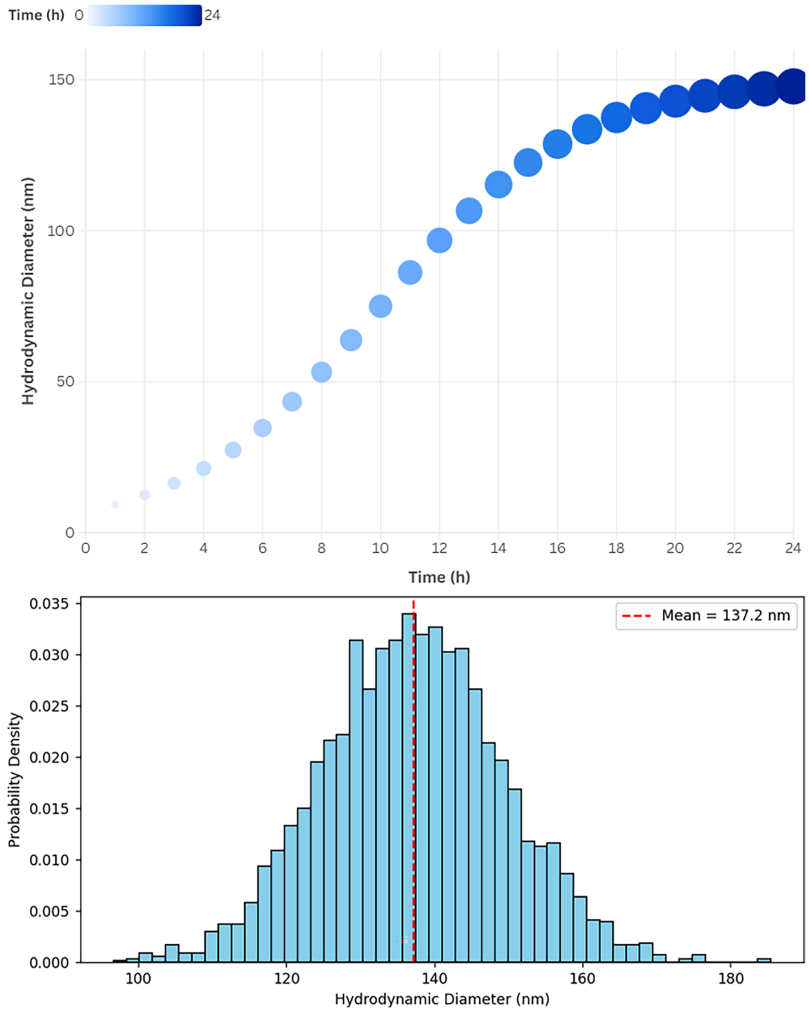

Figure 3. Time-dependent increase in hydrodynamic diameter of the peptide solution after BACE1 enzyme treatment, as measured by DLS. The particle size increased rapidly within the first 12 h and plateaued thereafter, indicating completion of self-assembly. Histogram of size distribution at 24 h shows a unimodal peak with an average diameter of 137.2 nm and a moderate spread, confirming uniform nanostructure formation

Figure 6: Compared to the control group, Aβ treatment alone induced a ~3.5-fold increase in IL-1β expression. Co-incubation with the inert peptide resulted in a moderate reduction (~2.8-fold), while the responsive peptide group showed a near-baseline expression (~1.4-fold), indicating strong suppression of the inflammatory response.

To further validate the enzyme-responsive nature of the peptide, HPLC analysis was conducted before and after incubation with BACE1. As shown in Figure 7, the major peak corresponding to the intact precursor (Rt = 18.3 min) was substantially reduced following enzymatic treatment. Simultaneously, two new peaks appeared at earlier retention times (Rt = 11.2 and 13.7 min), consistent with the expected cleavage products. These findings support the hypothesis that the BACE1 enzyme cleaves the ISEVKM recognition site within the peptide, triggering self-assembly via fragment exposure.

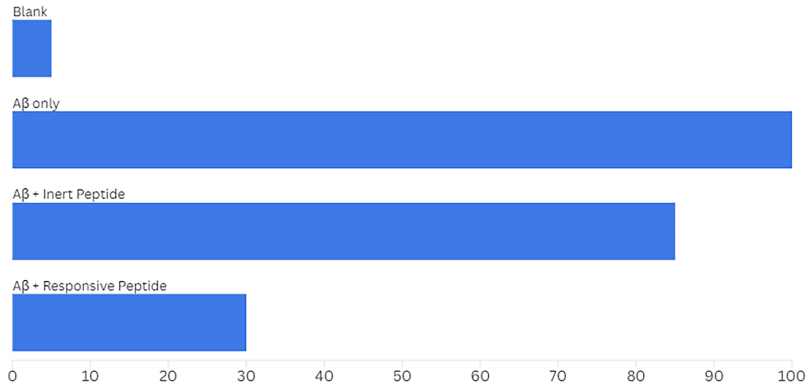

Figure 4. Thioflavin T (ThT) fluorescence intensity of Aβ solutions with or without peptide treatments. The presence of the responsive peptide significantly suppressed Aβ aggregation, as indicated by reduced ThT fluorescence, while the inert peptide showed limited effect. Data reflect mean fluorescence intensity after 24 h incubation

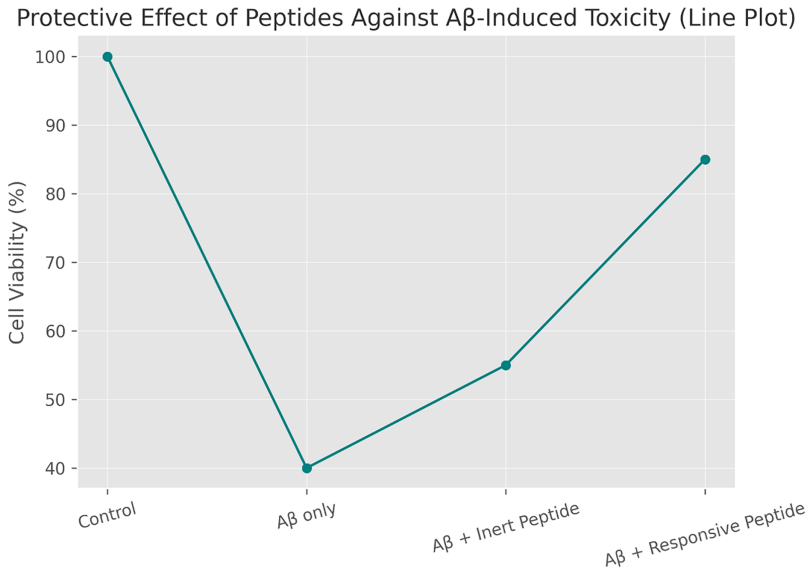

Figure 5. Cell viability (%) of neuronal cultures treated with Aβ and different peptides, measured by MTT assay. The responsive peptide markedly improved cell survival compared to Aβ alone or Aβ with inert peptide, indicating effective neuroprotection

4. Discussion

This strategy shown in Figure 1 leverages pathological enzyme activity for targeted self-assembly of functional nanofibers. By restricting activation to disease-relevant microenvironments, off-target effects are minimized. The formed nanostructures not only physically entrap Aβ but may also modulate local immune responses, providing a multifaceted approach to early neuroprotection in Alzheimer's disease.

Figure 2 demonstrates that the peptide self-assembly is specifically triggered by BACE1, a key enzyme involved in amyloid precursor protein cleavage. The strong scattering response reflects the formation of larger peptide nanostructures, validating the enzyme-responsiveness and selectivity of the design. This selective assembly mechanism ensures activation predominantly in Aβ-rich environments, supporting its potential for localized therapeutic intervention.

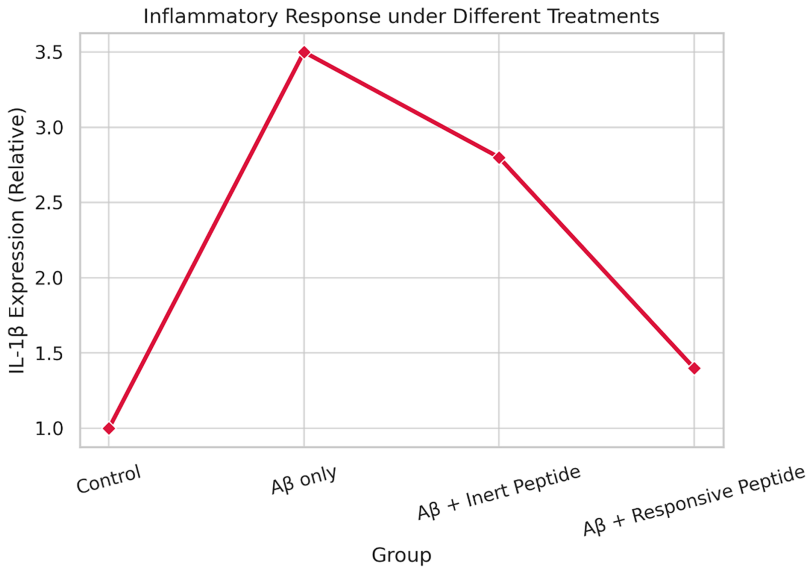

Figure 6. Relative expression levels of IL-1β in neuronal cultures treated with Aβ and different peptides. Aβ exposure significantly upregulated IL-1β expression, while co-treatment with the responsive peptide markedly reduced this proinflammatory response

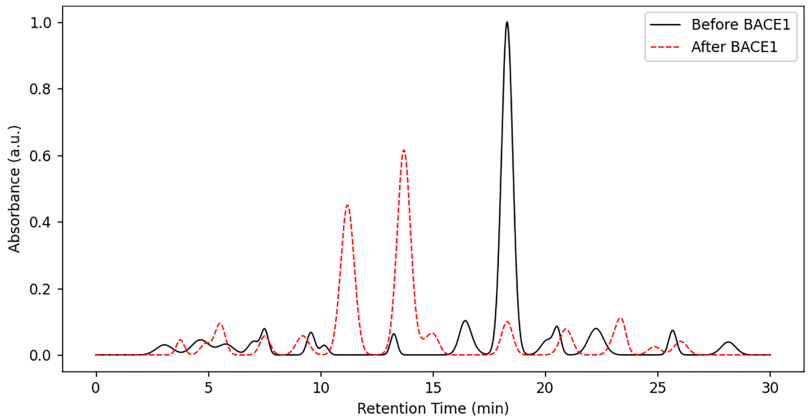

Figure 7. HPLC chromatograms of the responsive peptide before and after BACE1 enzyme treatment. A major peak at 18.3 min corresponding to the intact precursor peptide significantly decreased after incubation with BACE1, while two new peaks emerged at 11.2 min and 13.7 min, suggesting enzymatic cleavage and generation of peptide fragments. These results provide indirect evidence for BACE1-mediated covalent bond cleavage

This kinetic profile of Figure 3 provides strong evidence of enzyme-triggered peptide nanofiber formation. The initial lag phase likely corresponds to enzymatic cleavage and nucleation of primary aggregates, followed by accelerated growth through non-covalent interactions such as β-sheet stacking and hydrophobic packing. The plateau after ~18 h indicates a thermodynamic equilibrium state where further assembly is limited by depletion of monomer or structural stabilization. Such controlled and sustained self-assembly kinetics are advantageous for biomedical applications, allowing for spatial and temporal tuning of material formation within pathological microenvironments like Alzheimer's plaques. Importantly, the absence of abrupt aggregation minimizes the risk of toxicity often associated with uncontrolled peptide precipitation. These findings are further supported by the DLS size distribution histogram, which exhibits a single dominant peak centered at ~137 nm. The moderate PDI suggests that

the peptide assemblies maintain a relatively uniform population after enzymatic triggering. This degree of size homogeneity is favorable for potential biomedical applications such as controlled diffusion in neural tissues or efficient endocytosis in cell models

Figure 4 confirms the ability of the enzyme-responsive peptide to modulate Aβ aggregation behavior. The reduction in ThT signal is consistent with either inhibition of fibril elongation, disruption of nucleation pathways, or sequestration of Aβ monomers by the self-assembled nanostructures. Unlike inert analogs, the responsive peptide likely undergoes conformational transformation and assembles into nanofibers *in situ*, creating a local microenvironment that sterically or chemically interferes with Aβ self-association. This selective suppression of amyloidogenesis highlights the therapeutic potential of leveraging pathological enzyme cues to initiate functional nanomaterial formation directly at disease sites.

Figure 5 confirms the biofunctionality of the responsive peptide in a cellular model of Aβ-induced neurotoxicity. The high viability observed in the responsive peptide group suggests that the self-assembled nanofibers formed *in situ* mitigate Aβ's deleterious effects, either by physically sequestering toxic oligomers or by altering the local biochemical milieu. The superior performance compared to inert analogs highlights the importance of enzyme-triggered activation in conferring therapeutic specificity. These results support the concept of using pathological cues to drive functional nanostructure formation *in situ*, enabling localized and condition-specific neuroprotection with minimal off-target effects.

In Figure 6, the proinflammatory cytokine IL-1β plays a central role in neuroinflammation associated with Alzheimer's disease progression [25]. The elevated IL-1β level observed in the Aβ-only group reflects an inflammatory reaction induced by amyloid toxicity. While inert peptide offered some attenuation, the responsive peptide substantially mitigated the inflammatory response, supporting its functional activity in modulating cellular environments [26]. The nanofibers formed by enzymatic activation may sequester Aβ aggregates, reduce microglial activation, or physically shield cells from inflammatory triggers [27]. Importantly, the selective responsiveness to pathological enzymes allows inflammation modulation to occur specifically in disease contexts, minimizing off-target immunosuppression [28]. This highlights the dual therapeutic potential of the responsive peptide in both neuroprotection and neuroinflammation regulation [29].

Mechanistically, the system is designed to rely on covalent cleavage at the BACE1-recognizable site (ISEV↓KM), separating the peptide into two self-assembling fragments. Although direct MS-based fragment confirmation remains to be conducted, the shift in HPLC peaks before and after enzyme exposure (Figure 7) provides indirect but strong evidence for enzymatic scission. This cleavage-triggered design offers clear spatiotemporal control over assembly, making it distinct from non-covalent, environment-sensitive systems.

5. Conclusion

This study demonstrates the efficacy of an enzyme-responsive self-assembling peptide system for early intervention in Alzheimer's disease. The peptide remains inactive under normal conditions but undergoes targeted assembly into nanofibers in response to disease-associated enzymes such as BACE1. The resulting nanostructures effectively inhibit Aβ aggregation, reduce neurotoxicity, suppress inflammatory cytokine expression. Compared to inert analogs, the responsive peptide exhibits superior selectivity and functionality, underscoring the advantage of pathological environment–triggered activation. These findings highlight the promise of stimuli-responsive supramolecular biomaterials as a precise and multifunctional therapeutic strategy for neurodegenerative diseases.

Acknowledgement: Not applicable.

Funding Statement: The authors received no specific funding for this study.

Author Contributions: Yuanqing Song: Conceptualization, Methodology, Investigation, Data curation, Visualization, Writing—original draft. Yufan Liu: Supervision, Project administration, Resources,

Writing—review & editing, Funding acquisition. All authors reviewed the results and approved the final version of the manuscript.

Availability of Data and Materials: Data available on request from the authors.

Ethics Approval: Not applicable.

Conflicts of Interest: The authors declare no conflicts of interest to report regarding the present study.

Appendix A

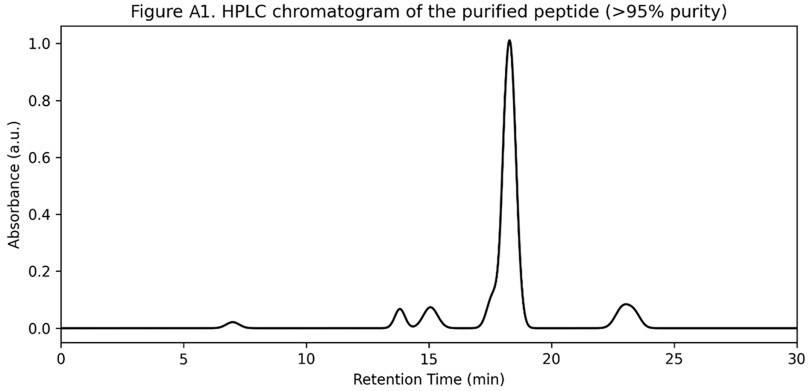

Figure A1. Analytical HPLC chromatogram of the purified peptide showing a single dominant peak (Rt = 18.3 min, >95% purity)

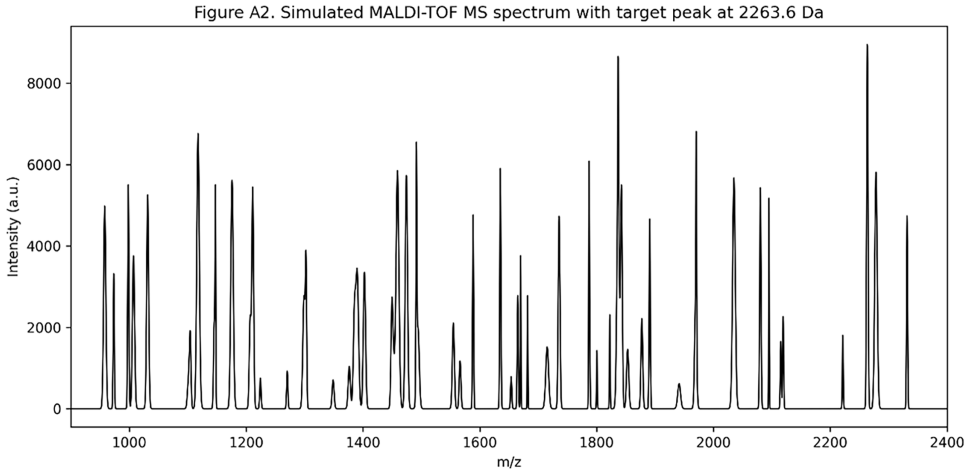

Figure A2. MALDI-TOF mass spectrum of the peptide, showing molecular ion peak at m/z = 2263.6 Da, matching the calculated molecular weight

References

1. Park KH, Oh EY, Han H, Kim JD, Kim SJ, Jeong KY, et al. Efficacy of transdermal immunotherapy with biodegradable microneedle patches in a murine asthma model. Clin Exp Allergy. 2020;50(9):1084–92. doi:10.1111/cea.13688.

2. Mirzaei F, Agbaria L, Bhatnagar K, Sirimanne N, Omar A'amar N, Jindal V, et al. Coffee and Alzheimer's disease. Prog Brain Res. 2024;289(1):21–55. doi:10.1016/bs.pbr.2024.06.002.
3. Lei X-L, Cheng K, Li Y, Zhong Z-T, Hou X-L, Song L-B, et al. The eradication of biofilm for therapy of bacterial infected chronic wound based on pH-responsive micelle of antimicrobial peptide derived biodegradable microneedle patch. Chem Eng J. 2023;462(3):142222. doi:10.1016/j.cej.2023.142222.
4. Prasad P, Gbadegesin O, Edwards M. Evolving management of Alzheimer's disease. J Neurol. 2024;271(12):7633–5. doi:10.1007/s00415-024-12720-7.
5. Kim H, Seong KY, Lee JH, Park W, Yang SY, Hahn SK. Biodegradable microneedle patch delivering antigenic peptide-hyaluronate conjugate for cancer immunotherapy. Acs Biom Sci Eng. 2019;5(10):5150–8. doi:10.1021/acsbiomaterials.9b00961.
6. Kirazov L, Dimitrova M. Mixed pathology and Alzheimer's disease. Acta Morphologica Et Anthropologica. 2024;31(3–4):42–7.
7. Lei X-L, Cheng K, Hu Y-G, Li Y, Hou X-L, Zhang F, et al. Gelatinase-responsive biodegradable targeted microneedle patch for abscess wound treatment of *S. aureus* infection. Int J Biol Macromol. 2023;253(Pt 8):127548. doi:10.1016/j.ijbiomac.2023.127548.
8. Kessing R. Alzheimer's disease: glymphatic system impaired. Fortschritte Der Neurologie Psychiatrie. 2024;1(1/2):4–5.
9. Kim HC, Tu R, Sodano HA. Aramid nanofibers-based multidimensional structure. Proc SPIE. 2023;12485:1248508. doi:10.1117/12.2658567.
10. Ain A-T-, Khatri A, Ali S, Ahmed F. Dope-dyed polyurethane electrospun nanofibers. J Text Inst. 2023;115(10):1899–905. doi:10.1080/00405000.2023.2271207.
11. Kandas I, Gamal M, Omran N, Noman S, Magdy G, Hassanin AH, et al. Nonlinear-optical piezoelectric electrospun nanofibers. Mat Res Bullet. 2024;171:112600. doi:10.1016/j.materresbull.2023.112600.
12. Przybyszewski AW, Chudzik A. How to cure Alzheimer's disease. J Alzheim Dis. 2024;99(4):1221–3. doi:10.3233/jad-240231.
13. Kim JH, Shin JU, Kim SH, Noh JY, Kim HR, Lee J, et al. Successful transdermal allergen delivery and allergen-specific immunotherapy using biodegradable microneedle patches. Biomaterials. 2018;150(Suppl):38–48. doi:10.1016/j.biomaterials.2017.10.013.
14. Qu M, Kim H-J, Zhou X, Wang C, Jiang X, Zhu J, et al. Biodegradable microneedle patch for transdermal gene delivery. Nanoscale. 2020;12(32):16724–9. doi:10.1039/d0nr02759f.
15. Castilla-Casadiego DA, Miranda-Muñoz KA, Roberts JL, Crowell AD, Gonzalez-Nino D, Choudhury D, et al. Biodegradable microneedle patch for delivery of meloxicam for managing pain in cattle. PLoS One. 2022;17(8):e0272169. doi:10.1371/journal.pone.0272169.
16. Guo X, Yan L, Zhang D, Zhao Y. Passive immunotherapy for Alzheimer's disease. Ageing Res Rev. 2024;94:102192. doi:10.1016/j.arr.2024.102192.
17. Li Y, Liu F, Su C, Yu B, Liu D, Chen HJ, et al. Biodegradable therapeutic microneedle patch for rapid antihypertensive treatment. Acs Appl Mat Interf. 2019;11(34):30575–84. doi:10.1021/acsami.9b09697.
18. Rajendran K, Krishnan UM. Biomarkers in Alzheimer's disease. Clin Chim Acta. 2024;562:119857. doi:10.1016/j.cca.2024.119857.
19. Shah V, Choudhury BK. Fabrication, physicochemical characterization, and performance evaluation of biodegradable polymeric microneedle patch system for enhanced transcutaneous flux of high molecular weight therapeutics. AAPS PharmSciTech. 2017;18(8):2936–48. doi:10.1208/s12249-017-0774-5.

20. Shin JU, Kim JD, Kim HK, Kang HK, Joo C, Lee JH, et al. The use of biodegradable microneedle patches to increase penetration of topical steroid for prurigo nodularis. Eur J Dermatol. 2018;28(1):71–7. doi:10.1684/ejd.2017.3164.
21. Song J-H, An EJ, Sung CY, Jeong DH, Lee G, Park S-Y. A comparative study on a biodegradable hyaluronic acid microneedle patch with a needleless patch for dry skin in atopic dermatitis: a single-blinded, split-body, randomized controlled trial. Arch Dermatol Res. 2023;315(3):569–81. doi:10.1007/s00403-022-02400-9.
22. Song J-H, An EJ, Sung CY, Jeong DH, Lee G, Park S-Y. Efficacy and safety of a biodegradable hyaluronic acid microneedle patch for dry skin in atopic dermatitis: a single-blinded, split-body, randomized controlled trial. J Korean Med Ophthalmol Otorhinolaryngol Dermatol. 2023;36(1):78–95.
23. Limenh LW. Advances in the transdermal delivery of antiretroviral drugs. Sage Open Med. 2024;12:20503121231223600. doi:10.1177/20503121231223600.
24. Stoeckel LE, Fazio EM, Hardy KK, Kidwiler N, Mclinden KA, Williams B. Clinically meaningful outcomes in Alzheimer's disease and Alzheimer's disease related dementias trials. Alzheimer's Dement -Transl Res Clin Interv. 2025;11(1):e70058. doi:10.1002/trc2.70058.
25. Tahmi M, Benitez R, Luchsinger J. Metformin as a potential prevention strategy for Alzheimer's disease and Alzheimer's disease related dementias. J Alzheimers Dis. 2024;101:S345–56. doi:10.3233/JAD-240495.
26. Tahmi M, Luchsinger JA. Metformin in the prevention of Alzheimer's disease and Alzheimer's disease related dementias. Jpad-J Prevent Alzheimers Dis. 2023;10(4):706–17. doi:10.14283/jpad.2023.113.
27. Wang S, Xie S, Zheng Q, Zhang Z, Wang T, Zhang G. Biofluid biomarkers for Alzheimer's disease. Front Aging Neurosci. 2024;16:1380237. doi:10.3389/fnagi.2024.1380237.
28. Testo AA, Roundy G, Dumas JA. Cognitive decline in Alzheimer's disease. Curr Top Behav Neurosci. 2025;69:181–95.
29. Walker LC, Jucker M. The prion principle and Alzheimer's disease: similarities to molecular mechanisms underlying prion diseases may help to refine Alzheimer's disease therapies. Science. 2024;385(6715):1278–9. doi:10.1126/science.adq5252.

Received: 01 July 2025; Accepted: 14 October 2025